



A Superconcentrated Water-in-Salt Hydrogel Electrolyte for High-Voltage Aqueous Potassium-Ion Batteries

Yibo Li⁺, Zhuqing Zhou⁺, Wenjun Deng, Chang Li, Xinran Yuan, Jun Hu, Man Zhang, Haibiao Chen, and Rui Li^{*[a]}

We report a high-voltage aqueous full potassium-ion battery (AFKIB) with a superconcentrated water-in-salt hydrogel electrolyte (WISHE). This WISHE exhibits an expanded electrochemical stability window (ESW) of 3.0 V as well as a high ionic conductivity of 4.34 mS cm⁻¹. The hydrogen bonds between the polymer network and the water phase help to further widen the ESW over a liquid-type water-in-salt electrolyte, and prevent liquid leakage. The assembled AFKIB exhibits a considerable capacity of 135 mA h g⁻¹ and a superior stability after 3000 cycles. This work provides a meaningful way of designing high-voltage aqueous energy storage devices.

Recently, concerns regarding the limited reserve of fossil fuels have stimulated the development and utilization of renewable energy sources, and active researches are focused on energy conversion and storage systems.^[1] Lithium-ion batteries offer high energy densities, but they still suffer from safety issues because of the flammable and toxic organic electrolytes.^[2] Aqueous electrolytes have received great attention because they are environmentally friendly, cheap, highly ionic conductivity and inherently safe.^[3] However, the narrow electrochemical stability window (ESW) of water (1.23 V) places a limit on the energy density of the aqueous batteries.^[4]

One effective method to break the ESW limit is to use water-in-salt electrolytes (WISE). Since the report of superconcentrated (21 m) lithium salt LiTFSI and its wide ESW, this electrolyte and its later improved derivatives have been widely studied and applied in high-voltage aqueous energy storage devices.^[5] In WISE, the water molecules strongly coordinate to cations (Li⁺, Na⁺, K⁺) and form solvent-sheath structures, leading to a decrease in the activity of the water and subsequently an expanded ESW beyond 1.23 V.^[5a,6] However, the cost and ionic conductivity can be issues for WISE with a very high salt concentration, and there is an intrinsic limit associated with liquid leakage.^[7]


Hydrogel electrolytes (HGEs) are widely used in flexible energy storage devices because they combine the strengths of solid and liquid electrolytes,^[8] and hydrogel has been proposed as a new carrier for WISE to prevent leakage.^[9] Nonetheless, traditional hydrogels are mostly based on dilute solutions, although there have been some recent reports of gel electrolytes with relatively high concentrations of lithium salts (≤ 10 mol kg⁻¹).^[10] The ESWs of these gel electrolytes remain narrow, which severely limit their applications in aqueous energy storage devices. Water-in-salt hydrogel electrolyte (WISHE) with a large number of hydroxyl, amino, and carboxyl groups can bind water molecules and further reduce the activity of water molecules ESW,^[11] thus, it could be a promising candidate in the development of high-voltage and safe aqueous electrolyte.^[12]

Herein, we successfully prepared a superconcentrated WISHE that contains 20 m potassium trifluoromethanesulfonate (KCF₃SO₃) and 30 m potassium bis(fluorosulfonyl)amide (KFSI). Such an ultrahigh concentration gel electrolyte is just like a solid electrolyte with excellent safety and stability as well as flexibility and high conductivity usually offered by a liquid electrolyte. An aqueous full K-ion battery (AFKIB) comprising KMnFe(CN)₆ (K-MnHCF) cathode, WISHE, and KTi₂(PO₄)₃/C (KTP/C) anode realizes a high operating voltage of 2.8 V and an ultra-long lifespan of 3000 charge-discharge cycles. Moreover, in the AFKIB, the KTP/C achieves a considerable capacity of 135 mA h g⁻¹ (close to theoretical capacity) and excellent rate capability. The operating voltage and durability of our AFKIB are better than that of the reported AFKIBs so far.^[6b,13] We believe that the demonstrated WISHE shows a new direction for the development of high-voltage and safe aqueous energy storage devices.

The above WISHE was synthesized via a facile one-step-heating process. Briefly, 20 mmol KCF₃SO₃ and 30 mmol KFSI were dissolved into 1.0 g deionized water to obtain a superconcentrated WISE (H₂O:K⁺ = 1.11:1 in molar ratio), then acrylamide was added and polymerized by heating at 80 °C for 30 minutes to produce the WISHE. To compare the ESWs between the traditional aqueous electrolyte, WISEs and the WISHE, we prepared 0.5 m K₂SO₄, 21 m KCF₃SO₃, 35 m KFSI, and (20 + 30) m WISEs. As shown in Figure 1a, the ESW of the 0.5 m K₂SO₄, 21 m KCF₃SO₃, 35 m KFSI, and (20 + 30) m WISEs are 0.99, 2.47, 2.55 and 2.77 V, respectively, by using Ti current collector in a two-electrode system. The wide ESWs of WISEs are attributed to the water molecules strongly coordinate to K⁺ ions, leading to a decrease in the activity of the water. The sharp peak at 3561 cm⁻¹ in the Raman spectra further

[a] Y. Li,⁺ Z. Zhou,⁺ Dr. W. Deng, C. Li, X. Yuan, J. Hu, M. Zhang, Prof. H. Chen, Prof. R. Li
School of Advanced Materials
Peking University Shenzhen Graduate School
Shenzhen, 518055, P. R. China
E-mail: liruisz@pku.edu.cn

[*] These authors contributed equally to this work

 Supporting information for this article is available on the WWW under <https://doi.org/10.1002/celec.202001509>

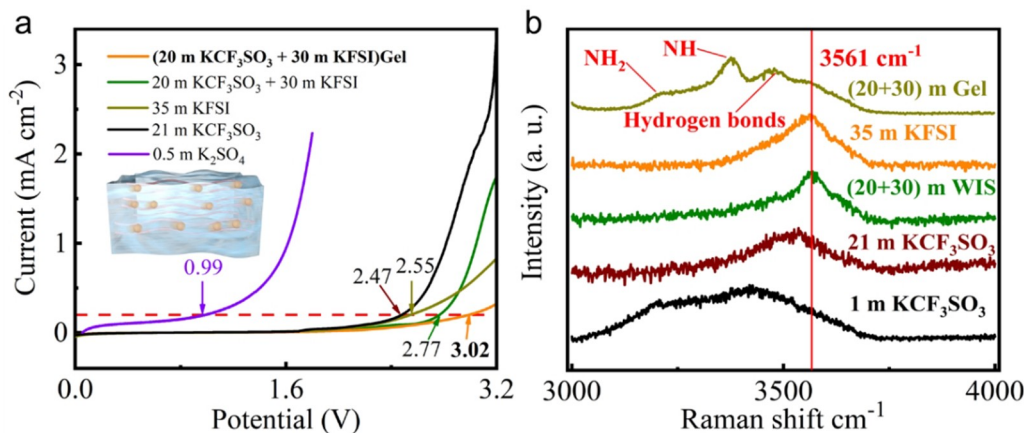


Figure 1. a) The electrochemical stability window of each electrolyte was measured by LSV between 0 V and 3.2 V by using a Ti//Ti two-electrode system at a scan rate of 10 mVs^{-1} and inset is the structural architecture of the Wishe. b) The Raman spectra of 1 m, 21 m KCF_3SO_3 , 35 m KFSI, (20+30) m WIS, and (20+30) m K-ion Wishe in the range of $3000\text{--}4000 \text{ cm}^{-1}$.

demonstrates the strong solvation of K^+ ions as shown in Figure 1b.^[6b] As for the Wishe, an even wider electrochemical stability window of 3.02 V was measured. Hydrogen bonds between the functional groups (N–H, N–H₂, C=O, and O–H bonds) and water molecules as observed by Raman at $3400\text{--}3500 \text{ cm}^{-1}$ are directly responsible for the expanded ESW and preventing the leakage of WISE.^[10b,14] And the NMR result (Figure S2) of (20+30) m WISE is consistent with the Raman analysis. The hydrogel polymer network will undergo a phase separation from the internal ions under an ultra-high ion concentration, resulting in a hierarchical framework for fast K-ion transport.^[2b,9b,15] As a result, a high ionic conductivity of 4.34 mS cm^{-1} (Figure S1) was measured in the Wishe with a superconcentrated WISE loaded. Figure S3 shows the digital image of the prepared Wishe, which is transparent with a diameter of 15.09 mm and a thickness of 0.99 mm. Moreover, the Wishe exhibits a superior stretchability and mechanical strength, stretched to above 600% strain (Figure S4). The mechanical properties attribute to the proper degree of cross-linking by specific crosslinking agents and high content of water.

To build a high-voltage AFKIB, Prussian Blue analogues K-MnHCF nanocubes were adopted as the cathode and synthesized via a simple modified co-precipitation method. The K-MnHCF has a high potential plateau benefitting from the high-spin $\text{Mn}^{\text{III}}/\text{Mn}^{\text{II}}\text{-N}$ couple, and the K-rich and low vacancy enable a theoretical specific capacity of 156 mAh g^{-1} .^[16] The X-ray diffraction (XRD) pattern of the K-MnHCF is shown in Figure 2a. All diffraction peaks agree well with K-MnHCF (PDF#51-1896), indicating high purity of the product. The morphology and structure of K-MnHCF were characterized by scanning electron microscopy (SEM) and transmission electron microscopy (TEM). SEM and TEM images (Figure 2b, 2c) show that the powder is composed of uniform nanocubes with a size of about $1 \mu\text{m}$. The high-resolution transmission electron microscopy (HRTEM) image is shown in Figure 2d and the calculated lattice fringe 0.505 nm is matching well with the interplanar spacing of the (200) planes of K-MnHCF.

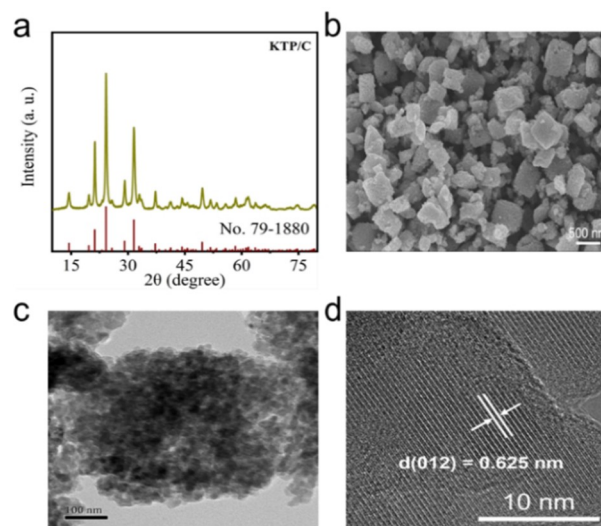


Figure 2. XRD pattern of K-MnHCF (a). SEM image (b), TEM image (c) and HRTEM image (d) of K-MnHCF with scale bars of 500 nm, 200 nm and 10 nm, respectively.

As for the anode candidates for aqueous K-ion batteries, they are hard to find because the large size of the K^+ cation always induces a substantial volume change in the anode material and causes irreversible structural degradation during (de)intercalation. Although NASICON-type $\text{KTi}_2(\text{PO}_4)_3$ (KTP) has a low specific capacity and poor rate capability in previously reported aqueous^[17] and nonaqueous^[18] system, it could be a promising electrode material owing to its robust 3D framework structure and appropriate K^+ insertion/extraction redox potential. Thus, we modified the KTP in this work by nanocrystallization and carbon coating. As shown in Figure 3a–c, the prepared product is very pure and it is made up of nanoparticles with a size of about $10\text{--}30 \text{ nm}$, after a hydrothermal reaction and a two-step annealing process. Larger particles size and porous structure are on account of secondary particles about $300\text{--}500 \text{ nm}$. Figure 3d shows the HRTEM image of the KTP/C and the calculated lattice fringe 0.625 nm is corresponding to the

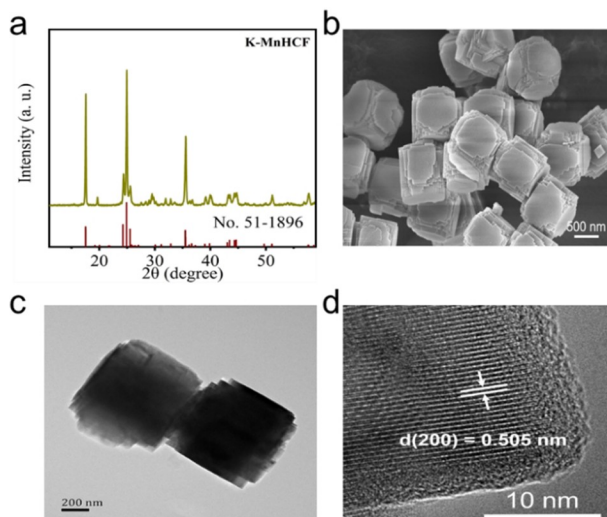


Figure 3. XRD pattern of KTP/C (a), SEM image (b), TEM image (c) and HRTEM image (d) of KTP/C with scale bars of 500 nm, 200 nm and 10 nm, respectively.

interplanar spacing of the (012) planes. In addition, a high electronic conductivity of KTP/C results from the compact amorphous carbon layer.

A “rocking-chair” type AFKIB was assembled with the above K-MnHCF cathode and KTP/C anode in a superconcentrated WISHE with the mass ratio of K-MnHCF: KTP/C is 3: 2. Figure 4a shows the long-term cycle performance of the AFKIB at a current density of 0.1 A g^{-1} . The initial Coulombic efficiency is 83.7% and the discharge capacity stabilizes rapidly at $\sim 135 \text{ mAh g}^{-1}$ (based on the anode active material, 21.5 mAh g^{-1} contributed by Ketjen Black conductive agents shown in Figure S6.) with a Coulombic efficiency of 94.3% after about 10 cycles. The reversible capacity retention is 98% after 100 cycles, indicating a high stability and reversibility. The initial capacity loss should be associated with the formation of a solid-electrolyte interface (SEI), which have been also observed in other fluorine-containing WISEs.^[5a,d] Such a high discharge capacity of KTP/C is attributed to its unique nanostructure and the expanded ESW allowing a deep discharge to insert more K^+ . The galvanostatic charge/discharge curves of the AFKIB (0.1 A g^{-1}) at different cycles are shown in Figure 4b with a low polarization even after 100 cycles, related to the high conductivity of the carbon layer. Excellent long-term cycling performance of this AFKIB was achieved with a capacity retention of 87.5% after 3000 cycles at 1.0 A g^{-1} (Figure 4c). As shown in Figure 4d, the discharge specific capacity decreases slowly as the rate increases, and the reversible capacities are 134.8, 118.8, 90.9 and 70.4 mAh g^{-1} at current densities of 0.1, 0.2, 0.5 and 1.0 A g^{-1} , respectively. When the current density

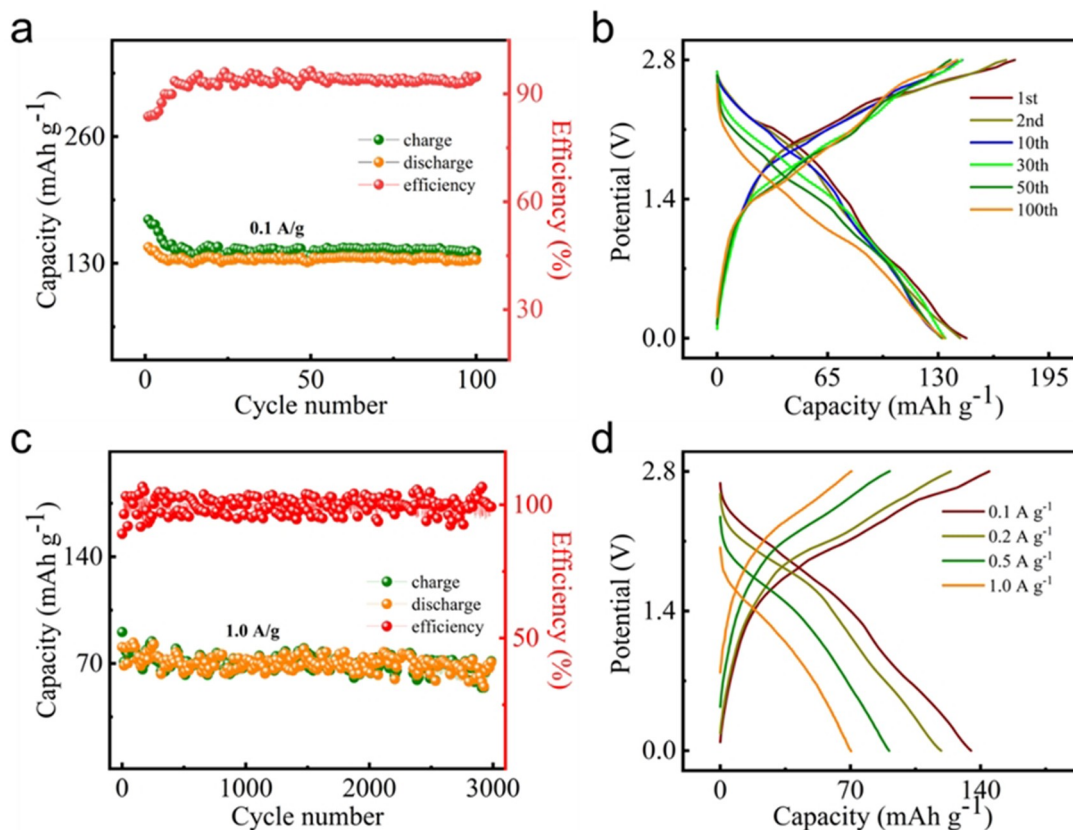


Figure 4. a) Long-term cycling performances of the full AKIB at a current density of 0.1 A g^{-1} and b) the corresponding charge/discharge curves of the full cell from 0 V to 2.8 V. c) Long cycle performances of the full cell at 1.0 A g^{-1} . d) Charge/discharge curves of K-MnHCF//KTP/C full cell at various current densities (0.1 to 1.0 A g^{-1}) in a voltage range of 0 to 2.8 V (all data are based on KTP/C).

returns to 0.1 Ag^{-1} , the discharge specific capacity recovers to the initial 135.5 mAhg^{-1} , implying a strong structural stability during the rapid K^+ (de)insertion (Figure S7). The high conductivity of the WISHE and the nanostructures and large ion channels in the K-MnHCF and KTP/C nanoparticles are also beneficial to the outstanding rate capability.

In summary, we report an ultrahigh concentration hydrogel electrolyte based on a superconcentrated WISE, providing an expanded electrochemical stability window of 3.0 V. This electrolyte enables a high-voltage and durable (3000 cycles) full aqueous potassium-ion battery. This water-in-salt hydrogel electrolyte not only inherits its advantages of WISE but also addresses the leakage problem. This work shares guidance for future aqueous electrolyte designs aiming at developing high-voltage and high-safety aqueous energy storage devices.

Acknowledgements

This work was supported by the Shenzhen Science and Technology Innovation Commission (JCYJ20180504165506495, JCYJ20170818085823773).

Conflict of Interest

The authors declare no conflict of interest.

Keywords: aqueous potassium-ion batteries · water-in-salt electrolytes · hydrogel electrolytes · superior capacity · high voltage

- [1] a) B. Dunn, H. Kamath, J.-M. Tarascon, *Science* **2011**, *334*, 928–935; b) D. P. Dubal, O. Ayyad, V. Ruiz, P. Gomez-Romero, *Chem. Soc. Rev.* **2015**, *44*, 1777–1790; c) F. Wang, X. Wu, X. Yuan, Z. Liu, Y. Zhang, L. Fu, Y. Zhu, Q. Zhou, Y. Wu, W. Huang, *Chem. Soc. Rev.* **2017**, *46*, 6816–6854.
- [2] a) Z. Yang, J. Zhang, M. C. Kintner-Meyer, X. Lu, D. Choi, J. P. Lemmon, J. Liu, *Chem. Rev.* **2011**, *111*, 3577–3613; b) C. Zhong, Y. Deng, W. Hu, J. Qiao, L. Zhang, J. Zhang, *Chem. Soc. Rev.* **2015**, *44*, 7484–7539.
- [3] a) J. Y. Luo, W. J. Cui, P. He, Y. Y. Xia, *Nat. Chem.* **2010**, *2*, 760–765; b) C. Liu, X. Wang, W. Deng, C. Li, J. Chen, M. Xue, R. Li, F. Pan, *Angew. Chem. Int. Ed.* **2018**, *57*, 7046–7050; c) T. Shao, C. Li, C. Liu, W. Deng, W. Wang, M. Xue, R. Li, *J. Mater. Chem. A* **2019**, *7*, 1749–1755; d) B. Scrosati, J. Hassoun, Y.-K. Sun, *Energy Environ. Sci.* **2011**, *4*, 3287–3295.
- [4] a) H. Kim, J. Hong, K. Y. Park, H. Kim, S. W. Kim, K. Kang, *Chem. Rev.* **2014**, *114*, 11788–11827; b) A. Ramanujapuram, D. Gordon, A. Magasinski, B. Ward, N. Nitta, C. Huang, G. Yushin, *Energy Environ. Sci.* **2016**, *9*, 1841–1848.
- [5] a) L. Suo, O. Borodin, T. Gao, M. Olguin, J. Ho, X. Fan, C. Luo, C. Wang, K. Xu, *Science* **2015**, *350*, 938–943; b) Y. Yamada, K. Usui, K. Sodeyama, S. Ko, Y. Tateyama, A. Yamada, *Nat. Energy* **2016**, *1*, 16129–16138; c) D. Xiao, Q. Dou, L. Zhang, Y. Ma, S. Shi, S. Lei, H. Yu, X. Yan, *Adv. Funct. Mater.* **2019**, *29*, 1904136; d) L. Suo, D. Oh, Y. Lin, Z. Zhuo, O. Borodin, T. Gao, F. Wang, A. Kushima, Z. Wang, H. C. Kim, Y. Qi, W. Yang, F. Pan, J. Li, K. Xu, C. Wang, *J. Am. Chem. Soc.* **2017**, *139*, 18670–18680; e) W. Deng, X. Wang, C. Liu, C. Li, J. Chen, N. Zhu, R. Li, M. Xue, *Energy Storage Mater.* **2019**, *20*, 373–379; f) Z. Tian, W. Deng, X. Wang, C. Liu, C. Li, J. Chen, M. Xue, R. Li, F. Pan, *Funct. Mater. Lett.* **2018**, *10*, 1750081; g) H. Bi, X. Wang, H. Liu, Y. He, W. Wang, W. Deng, X. Ma, Y. Wang, W. Rao, Y. Chai, H. Ma, R. Li, J. Chen, Y. Wang, M. Xue, *Adv. Mater.* **2020**, *32*, 2000074.
- [6] a) H. Zhang, B. Qin, J. Han, S. Passerini, *ACS Energy Lett.* **2018**, *3*, 1769–1770; b) L. Jiang, Y. Lu, C. Zhao, L. Liu, J. Zhang, Q. Zhang, X. Shen, J. Zhao, X. Yu, H. Li, X. Huang, L. Chen, Y.-S. Hu, *Nat. Energy* **2019**, *4*, 495–503.
- [7] M. Yu, Y. Lu, H. Zheng, X. Lu, *Chemistry* **2018**, *24*, 3639–3649.
- [8] a) H. Yuk, B. Lu, X. Zhao, *Chem. Soc. Rev.* **2019**, *48*, 1642–1667; b) L. Fang, Z. Cai, Z. Ding, T. Chen, J. Zhang, F. Chen, J. Shen, F. Chen, R. Li, X. Zhou, Z. Xie, *ACS Appl. Mater. Interfaces* **2019**, *11*, 21895–21903.
- [9] a) X. Hou, W. Guo, L. Jiang, *Chem. Soc. Rev.* **2011**, *40*, 2385–2401; b) W. Liu, S. W. Lee, D. Lin, F. Shi, S. Wang, A. D. Sendek, Y. Cui, *Nat. Energy* **2017**, *2*, 17035.
- [10] a) J. Zhou, D. Wu, C. Wu, G. Wei, J. Wei, Z. Tai, S. Xi, S. Shen, Q. Wang, Y. Chen, *J. Mater. Chem. A* **2019**, *7*, 19753–19760; b) L. Dai, O. Arcelus, L. Sun, H. Wang, J. Carrasco, H. Zhang, W. Zhang, J. Tang, *J. Mater. Chem. A* **2019**, *7*, 24800–24806; c) Q. Liu, J. Zhou, C. Song, X. Li, Z. Wang, J. Yang, J. Cheng, H. Li, B. Wang, *Energy Storage Mater.* **2020**, *24*, 495–503; d) J. M. Park, M. Jana, P. Nakhaneve, B.-K. Kim, H. S. Park, *ACS Energy Lett.* **2020**, *5*, 1054–1061.
- [11] a) W. Zhang, P. Feng, J. Chen, Z. Sun, B. Zhao, *Prog. Polym. Sci.* **2019**, *88*, 220–240; b) D. Caccavo, S. Cascone, G. Lamberti, A. A. Barba, *Chem. Soc. Rev.* **2018**, *47*, 2357–2373.
- [12] Z. Wang, H. Li, Z. Tang, Z. Liu, Z. Ruan, L. Ma, Q. Yang, D. Wang, C. Zhi, *Adv. Funct. Mater.* **2018**, *28*, 1804560.
- [13] H. Chen, Z. Zhang, Z. Wei, G. Chen, X. Yang, C. Wang, F. Du, *Sustain. Energy Fuels* **2020**, *4*, 128–131.
- [14] E. S. Dragan, M. M. Perju, M. V. Dinu, *Carbohydr. Polym.* **2012**, *88*, 270–281.
- [15] Y. Huang, M. Zhong, Y. Huang, M. Zhu, Z. Pei, Z. Wang, Q. Xue, X. Xie, C. Zhi, *Nat. Commun.* **2015**, *6*, 10310.
- [16] L. Xue, Y. Li, H. Gao, W. Zhou, X. Lu, W. Kaveevitvachai, A. Manthiram, J. B. Goodenough, *J. Am. Chem. Soc.* **2017**, *139*, 2164–2167.
- [17] D. P. Leonard, Z. Wei, G. Chen, F. Du, X. Ji, *ACS Energy Lett.* **2018**, *3*, 373–374.
- [18] J. Han, Y. Niu, S. J. Bao, Y. N. Yu, S. Y. Lu, M. Xu, *Chem. Commun.* **2016**, *52*, 11661–11664.

Manuscript received: November 26, 2020
 Revised manuscript received: January 21, 2021
 Accepted manuscript online: January 26, 2021